

Continuing global significance of emissions of Montreal Protocol–restricted halocarbons in the United States and Canada

D. F. Hurst,^{1,2} J. C. Lin,^{3,4} P. A. Romashkin,^{1,2,5} B. C. Daube,³ C. Gerbig,^{3,6}
D. M. Matross,³ S. C. Wofsy,³ B. D. Hall,² and J. W. Elkins²

Received 19 October 2005; revised 9 February 2006; accepted 5 April 2006; published 4 August 2006.

[1] Contemporary emissions of six restricted, ozone-depleting halocarbons, chlorofluorocarbon-11 (CFC-11, CCl₃F), CFC-12 (CCl₂F₂), CFC-113 (CCl₂FCClF₂), methyl chloroform (CH₃CCl₃), carbon tetrachloride (CCl₄), and Halon-1211 (CBrClF₂), and two nonregulated trace gases, chloroform (CHCl₃) and sulfur hexafluoride (SF₆), are estimated for the United States and Canada. The estimates derive from 900 to 2900 in situ measurements of each of these gases within and above the planetary boundary layer over the United States and Canada as part of the 2003 CO₂ Budget and Regional Airborne–North America (COBRA-NA) study. Air masses polluted by anthropogenic sources, identified by concurrently elevated levels of carbon monoxide (CO), SF₆, and CHCl₃, were sampled over a wide geographical range of these two countries. For each polluted air mass, we calculated emission ratios of halocarbons to CO and employed the Stochastic Time-Inverted Lagrangian Transport (STILT) model to determine the footprint associated with the air mass. Gridded CO emission estimates were then mapped onto the footprints and combined with measured emission ratios to generate footprint-weighted halocarbon flux estimates. We present statistically significant linear relationships between halocarbon fluxes (excluding CCl₄) and footprint-weighted population densities, with slopes representative of per capita emission rates. These rates indicate that contemporary emissions of five restricted halocarbons (excluding CCl₄) in the United States and Canada continue to account for significant fractions (7–40%) of global emissions.

Citation: Hurst, D. F., J. C. Lin, P. A. Romashkin, B. C. Daube, C. Gerbig, D. M. Matross, S. C. Wofsy, B. D. Hall, and J. W. Elkins (2006), Continuing global significance of emissions of Montreal Protocol–restricted halocarbons in the United States and Canada, *J. Geophys. Res.*, *111*, D15302, doi:10.1029/2005JD006785.

1. Introduction

[2] The Montreal Protocol on Substances that Deplete the Ozone Layer and its Amendments and Adjustments (hereinafter called the Montreal Protocol) have effected sizable reductions in the global production and emissions of many ozone-depleting substances (ODSs) since the late 1980s. Initial observations of decreasing atmospheric growth rates for several ODSs [e.g., Elkins *et al.*, 1993; Montzka *et al.*, 1996; Cunnold *et al.*, 1997; Simmonds *et al.*, 1998] have now been updated by reports of declining burdens of ozone-depleting chlorine and bromine in the atmosphere [e.g.,

Montzka *et al.*, 1999; Prinn *et al.*, 2000; Montzka and Fraser, 2003; Montzka *et al.*, 2003]. These observations clearly illustrate the efficacy of the Montreal Protocol in rapidly and significantly reducing global ODS emissions as a first step toward the recovery of stratospheric ozone.

[3] The six restricted halocarbons studied here are man-made chemicals with ozone depletion potentials (ODPs) ranging from 0.12 (CH₃CCl₃) to 6.0 (Halon-1211) and atmospheric lifetimes ranging from ~5 yr (CH₃CCl₃) to ~100 yr (CFC-12) [Montzka and Fraser, 2003]. Their principal applications were refrigeration (CFC-12), foam blowing (CFC-11), electronics deflusing and cleaning (CFC-113), fire extinguishing (Halon-1211), metal degreasing (CH₃CCl₃), and serving as the feedstock for CFC-11 and CFC-12 production (CCl₄). Only CH₃CCl₃ is emitted in significant quantities by nonindustrial sources (biomass fires), although 75–95% of its modern global emissions are attributed to anthropogenic sources [Rudolph *et al.*, 2000].

[4] The Montreal Protocol first mandated reductions in ODS manufacture in non-Article 5 (developed) countries which, in 1989, accounted for 93–98% of the world's production of CFCs, halons, and CH₃CCl₃, and 73% of global CCl₄ manufacture [United Nations Environment

¹Cooperative Institute for Research in Environmental Sciences, University of Colorado, Boulder, Colorado, USA.

²Global Monitoring Division, NOAA Earth System Research Laboratory, Boulder, Colorado, USA.

³Department of Earth and Planetary Sciences and Division of Engineering and Applied Sciences, Harvard University, Cambridge, Massachusetts, USA.

⁴Now at Department of Earth Sciences, University of Waterloo, Waterloo, Ontario, Canada.

⁵Now at Research Aviation Facility, National Center for Atmospheric Research, Broomfield, Colorado, USA.

⁶Now at Max Planck Institute for Biogeochemistry, Jena, Germany.

Programme (UNEP), 2002a] (see www.unep.org/ozone/15-year-data-report.pdf). It should be noted here that *UNEP* [2002a] production figures for CCl_4 exclude amounts made as feedstock for CFC production. Deadlines for the phase-out of ODS production in developed nations were 1 January 1994 for halons and 1 January 1996 for CFCs, CH_3CCl_3 and CCl_4 . In response, production of CFCs, halons, and CH_3CCl_3 in developed nations reportedly decreased by 95–99% during 1989–1996, driving 76–98% reductions in their worldwide production [*UNEP*, 2002a]. Global production figures for CCl_4 became negative during this same period because greater amounts were destroyed than produced [*UNEP*, 2002a].

[5] Global manufacture of these ODSs continued after 1995 because the Montreal Protocol permits their production in Article 5 (developing) countries until 2010 (2015 for CH_3CCl_3) and because a limited amount of manufacture was sustained in developed countries for exempted uses and small-scale export to developing nations. During 1996–2000, global production of CFCs and CH_3CCl_3 remained fairly steady at 12–15% and 2–3% of 1989 levels, respectively, while halon production decreased another 15% (down to 9% of 1989 levels) [*UNEP*, 2002a, 2002b]. Additional production cutbacks during 2001–2003 further diminished global manufacture (in 2003) to 8% (CFCs), 3% (halons), and 1% (CH_3CCl_3) of 1989 levels [*UNEP*, 2005].

[6] The United States was the leading global manufacturer of ODSs until the mid-1990s when the bulk of worldwide production shifted from developed to developing countries [*UNEP*, 2002a]. Between 1986 and the mid-1990s, U.S. production figures cumulatively accounted for 27–29% of the reported global manufacture of CFCs and halons, 45% of CH_3CCl_3 , and 16% of nonfeedstock CCl_4 [*UNEP*, 2002a]. Canadian production figures reported for the same period were 1.4% (CFCs), 0% (halons), 0.7% (CH_3CCl_3), and 8% (CCl_4) of worldwide totals.

[7] Global emissions of these six ODSs, as depicted in the halocarbon emission scenario Ab [*Montzka and Fraser*, 2003], diminished by 50% (ODP-weighted sum) from 1989 through 1993, very similar to the relative decrease in their reported global production during that period [*UNEP*, 2002a]. Between 1994 and 1996, however, the decline in emissions slowed abruptly relative to the continued rapid decrease in global production. By 2002, the ODP-weighted global emissions of these chemicals had fallen only 74% from their 1989 values compared to a 93% decrease in their ODP-weighted production [*Montzka and Fraser*, 2003; *UNEP*, 2002a, 2004]. This difference attested to significant global emissions of previously produced ODSs held in reservoirs (banks) such as older refrigerators and air conditioners, fire extinguishing systems, blown foam products, and stockpiles intended for the future servicing of older equipment. On the basis of the history of national ODS production figures, developed countries should have held the preponderance of global banks before their manufacture was greatly curtailed in the mid-1990s. It is quite uncertain how banks have evolved since that time.

[8] The importance of banks to contemporary and future global emissions of CFCs and halons is clearly revealed by global emission estimates that have exceeded global production figures since the mid-1990s [*Montzka and Fraser*, 2003; *UNEP*, 2002a, 2002b, 2003b, 2004, 2005]. Given this

importance, accurate projections of future ODS emissions require accurate estimates of the sizes and emissions of modern ODS banks. Bank sizes can be calculated as the sums of annual differences between global production and emissions, but any persistent biases in production or emission figures can lead to large cumulative biases in the bank size estimates. A different approach is to compile global inventories of equipment and products containing ODSs [*Intergovernmental Panel on Climate Change/Technology and Economic Assessment Panel (IPCC/TEAP)*, 2005]. Differences between the two methods are apparent in their discrepant estimates of the modern global bank of CFCs, ~ 720 Gg in 2000 [*Montzka and Fraser*, 2003] and ~ 2400 Gg in 2002 [*IPCC/TEAP*, 2005].

[9] Global ODS emissions have typically been estimated by two independent methods. The first is an inventory-based method where emissions are deduced from records of reported production/sales and estimated release functions that describe the delays between manufacture and emission to the atmosphere of ODSs based on their various uses [e.g., *Midgley and McCulloch*, 1995; *McCulloch and Midgley*, 2001; *McCulloch et al.*, 2001, 2003]. Release functions were undoubtedly more predictable before 1996 when emissions in developed countries were more closely linked to production and sales. The second is a burden-based method where emissions are determined from the atmospheric lifetimes of these chemicals and measured changes in their atmospheric burdens. Agreement between the two estimation methods has ranged from excellent to poor, with the latter illustrated by inventory-based estimates of CFC-11, CFC-113, and Halon-1211 emissions for 1994–2000 that were 50–80% of the burden-based estimates [*Montzka and Fraser*, 2003]. A recent set of global emission estimates for 2002 has reduced inventory-based emissions of CFC-11 to only 30–40% of the burden-based estimate and increased inventory-based Halon-1211 emissions to twice the burden-based estimate [*IPCC/TEAP*, 2005]. Any biases in annual emission estimates resulting from errors in release functions or atmospheric lifetimes will propagate cumulative biases in bank size estimates over time.

[10] Numerous studies of ODS emissions have been conducted, predominantly in developed countries, to provide important checks of the inventory- and burden-based estimates of global emissions. Specifically, ODS emissions have been estimated at regional to continental scales from measurements made at remote, ground-based sites influenced by episodic pollution from distant sources [e.g., *Prather*, 1985; *Bakwin et al.*, 1997; *Derwent et al.*, 1998; *Simmonds et al.*, 1998; *Ryall et al.*, 2001; *Barnes et al.*, 2003; *Millet and Goldstein*, 2004; *Li et al.*, 2005], as well as from mobile measurement platforms such as aircraft or trains [e.g., *Krol et al.*, 2003; *Palmer et al.*, 2003; *Hurst et al.*, 2004].

[11] In this work we estimate contemporary anthropogenic emissions of six restricted halocarbons in the United States and Canada and assess their global significance more than 7 years after production ceased. The estimates are based on thousands of in situ measurements of these gases, made from a small aircraft as it flew over many different regions of these two countries and intermittently intercepted polluted air masses. For each polluted air mass that was sampled we calculated emission ratios of halocarbons to CO and

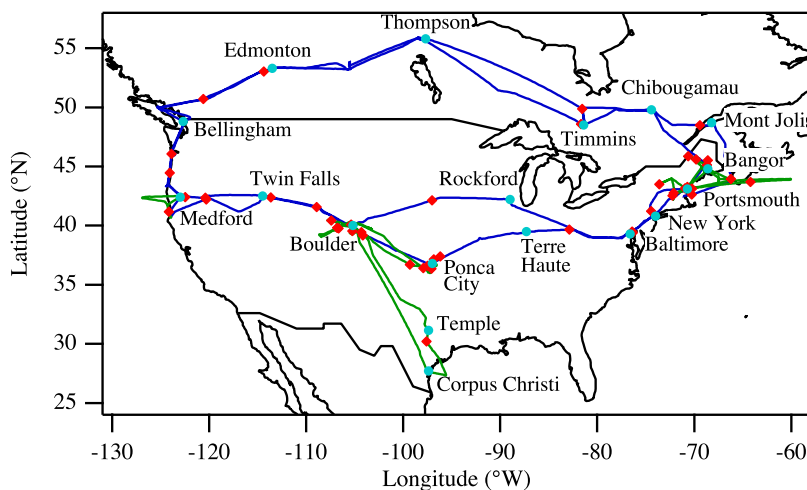


Figure 1. Flight tracks for the 38 flights of the Cessna Citation II jet aircraft during the 2003 COBRA-NA campaign. Green tracks depict regional survey flights where the aircraft returned daily to the point of origin. Blue tracks portray point-to-point flights that constructed two transcontinental circuits (26 May to 12 June, 18–28 June) which started and finished in Boulder, Colorado. Differences between the two clockwise circuits include the earlier circuit's more southerly track into Timmins, Ontario, and more northerly routes through Mont Joli, Quebec, to Portsmouth, New Hampshire, and through Rockford, Illinois, to Boulder. The aircraft landed at city airports (cyan circles) and intercepted the polluted air masses analyzed in this work at 45 different locations (red diamonds).

employed a transport model to associate the measured pollution with a source region depicted as a footprint. Footprint-weighted mean fluxes of CO and the six restricted halocarbons were calculated, then related to footprint-weighted mean population densities to determine per capita emissions of each halocarbon. The per capita emissions were scaled by population into estimates of halocarbon emissions in the United States and Canada during 2003.

2. Methods

2.1. Study

[12] The COBRA-NA study was designed to provide comprehensive vertical profile measurements of carbon dioxide (CO₂) and other radiatively important trace gases to test modeling concepts that aim to quantify surface-atmosphere fluxes on the basis of inverse methods. The study was conducted from 23 May to 28 June 2003 aboard the University of North Dakota's Cessna Citation II twin-engine jet aircraft. A total of 38 flight legs of ≤ 4 hour duration were flown (Figure 1), with two legs normally completed each flight day.

[13] Two types of flights were conducted for this study: regional flights with frequent vertical soundings to and from locations 150–1500 km away from our aircraft bases in Boulder, Colorado, and Portsmouth, New Hampshire, and point-to-point flights with less frequent vertical soundings that comprised two $\sim 11,000$ km transcontinental circuits across the United States and Canada. Regional flights were designed to measure trace gas concentration changes as air masses traveled across the landscape, enabling determinations of regional fluxes in a Lagrangian framework [Lin *et al.*, 2004]. Circuit flights were intended to survey trace gas distributions in the horizontal and vertical over large regions of the United States and

Canada. The near-field sampling of pollution plumes from large population centers was not a primary objective of this campaign. Though the airports required for aircraft refueling were in populated areas, the polluted air masses sampled during flights were generally encountered at considerable distances from cities.

2.2. Measurements

[14] The aircraft was outfitted with a 22.5 mm ID, ram-pressure-fed, aluminum inlet and flow-through manifold to provide a rapidly flowing stream of outside air to the instruments. Each instrument drew air from an independent port in the manifold through its own sampling line and pump. In situ instrumentation aboard the aircraft (Table 1) included a custom-built four-channel gas chromatograph (GC), the Airborne Chromatograph for Atmospheric Trace Species (ACATS-IV) [Elkins *et al.*, 1996; Romashkin *et al.*, 2001] and a modified commercial CO instrument (Aero-Laser GmbH, Germany) based on the vacuum-ultraviolet fluorescence (VUVF) technique [Gerbig *et al.*, 1999]. These instruments were calibrated in flight using high-pressure cylinders of dried, whole air that were standardized against the calibration scales of the NOAA Global Monitoring Division (GMD, formerly CMDL). ACATS-IV was calibrated every 560 s and the CO instrument every 30 min. Pertinent details about the measurements, in-flight precision and data intervals for these two instruments are presented (Table 1). Other instrumentation onboard included a custom-built nondispersive infrared (NDIR) analyzer for CO₂ [Daube *et al.*, 2002], a global positioning system to determine aircraft location (Applanix, Canada), and commercial sensors for outside air temperature, static pressure, and other meteorological parameters (Rosemount Inc., United States).

[15] Data obtained during aircraft taxi and during final approaches of the aircraft into airports were not used in this

Table 1. COBRA-NA Measurement Statistics^a

Chemical	Instrument ^b	Data Interval ^c	Number of Measurements	Mean χ^d	95% χ^d	Mean Precision	
						χ^d	Percent ^e
CFC-11	ACATS	140	997	257.4	259.4	1.5	0.6
CFC-12	ACATS	70	2565	534.8	540.2	3.8	0.7
CFC-113	ACATS	140	903	81.3	82.1	0.6	0.7
CH ₃ CCl ₃	ACATS	140	976	23.2	24.5	0.7	3.2
CCl ₄	ACATS	140	939	97.8	98.6	0.7	0.7
Halon-1211	ACATS	70	2206	4.41	4.57	0.08	1.8
CHCl ₃	ACATS	140	962	11.7	15.0	0.6	5.1
SF ₆	ACATS	70	2925	5.36	5.57	0.07	1.3
CO	VUVF	1	263,010	142	202	2	1.4

^aTable values reflect measurements made after initial climb, before final approach, and outside of air masses significantly influenced by biomass fire emissions (see sections 2.2 and 2.3).

^bACATS is the four-channel Airborne Chromatograph for Atmospheric Trace Species of NOAA/ESRL/GMD. VUVF is the vacuum-ultraviolet fluorescence instrument of Harvard University.

^cData interval (in seconds) excludes periods of calibration (see section 2.2).

^dMixing ratios (dry mole fractions) corresponding to the mean, 95th percentile, and mean precision values for measurements are given in units of parts per trillion (10^{12} , ppt) except for CO, which is given in units of parts per billion (10^9 , ppb).

^eMean precision relative to mean mixing ratio.

study because of strong influences from local airport-based sources. We also discarded GC measurements made during the initial aircraft climb from airports because they were generally of poorer precision and more susceptible to contamination of the manifold, sampling lines, and pumps by airport-generated pollution and minuscule leaks of contaminated cabin air into the sampling systems while on the ground. The aircraft cabin and sampling systems were adequately flushed with clean air by the time the aircraft concluded its initial climb, typically 10–15 min into the flight, at which time the GC had properly warmed up and stabilized.

[16] The COBRA-NA measurements provide a unique, geographically extensive data set that is beneficial to determinations of large-scale emissions of trace gases, especially those with poorly known source distributions. During the era of ODS production, halocarbon sources were ubiquitous in developed countries and estimates of their large-scale emissions based on measurements at only 1–2 fixed sites were justifiable. Now, grand spatial extrapolations of restricted halocarbon emission estimates based on measurements at only a few locations may no longer be reliable because so little is known about their modern source distributions. The COBRA-NA data set permits large-scale emissions to be determined without relying on potentially precarious spatial extrapolations. Our estimates provide important checks of the representativeness of emission estimates from measurements at fixed sites in the United States and Canada, but the short duration of the COBRA-NA study cannot address seasonal and longer-term trends in emissions that are readily available from continual, long-term measurements at fixed sites.

2.3. Identification and Characterization of Anthropogenic Pollution Plumes

[17] The initial step in estimating anthropogenic emissions of the six restricted halocarbons was to identify the air masses polluted by anthropogenic sources, hereinafter referred to as polluted air masses. Once identified, polluted air masses were characterized by calculating emission ratios relative to CO from the measurement data obtained within them.

[18] Concurrent measurements of two anthropogenic tracers, SF₆ and CO, were used to identify air masses that were polluted. Sulfur hexafluoride is used as a dielectric in high-voltage electrical power distribution equipment [Maiss *et al.*, 1996; Geller *et al.*, 1997; Maiss and Brenninkmeijer, 1998], is strictly anthropogenic in origin, and has an atmospheric lifetime (τ) of >800 years [Morris *et al.*, 1995]. Carbon monoxide is emitted during the combustion of fossil fuels and biomass, is produced by the oxidation of methane (CH₄) and nonmethane hydrocarbons (NMHCs), and has a globally averaged lifetime of \sim 2 months [e.g., Logan *et al.*, 1981]. Neither gas is regulated by the Montreal Protocol, and there is typically good correlation between their mixing ratios in anthropogenically influenced air masses [e.g., Bakwin *et al.*, 1997]. Coincident, rapid increases and subsequent decreases in their mixing ratios should therefore be a good indication that a polluted air mass was sampled. An example of sampling polluted air (Figure 2) also portrays concurrent increases and decreases in CFC-12 mixing ratios, but we refrained from using elevated mixing ratios of restricted halocarbons for identification because they might introduce bias in our analysis by excluding polluted air devoid of recently emitted restricted halocarbons.

[19] Measurements of another nonregulated anthropogenic tracer, CHCl₃, were employed to corroborate the SF₆- and CO-based identification of polluted air masses. Chloroform ($\tau \approx$ 6 months) is emitted by pulp and paper manufacture (\sim 50% of anthropogenic emissions), water and waste treatment (\sim 30%), other industrial processes (\sim 15%), and combustion (<1%) [Aucott *et al.*, 1999]. Though CHCl₃ contains chlorine, its production is not regulated by the Montreal Protocol because of its short atmospheric lifetime. Though the vast majority of CHCl₃ emanates from natural sources in oceans and soils [Khalil *et al.*, 1999], these emissions are very diffuse relative to anthropogenic point sources and should not strongly influence singular air masses. The same holds true for the significant amounts of CO produced by the oxidation of CH₄ and nonanthropogenic NMHCs.

[20] Emissions from biomass fires significantly increased the CO and CHCl₃ mixing ratios in air masses sampled

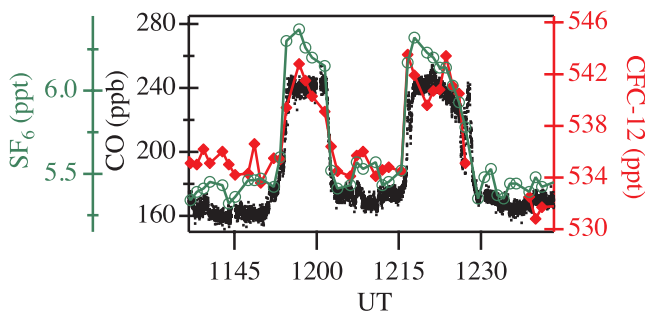


Figure 2. Time series of CO (black), CFC-12 (red), and SF₆ (green) mixing ratios measured in northern central Massachusetts during a regional survey flight from Portsmouth, New Hampshire, on 6 June 2003. Two air masses containing elevated mixing ratios of these three gases were sampled. The first was sampled between 0750 and 0802 local time (1150 and 1202 UT) as the aircraft descended from 1000 to 180 m altitude, flew level for 5 min, then climbed back to 800 m altitude. At 0817 local time (1217 UT) the aircraft again descended into the planetary boundary layer to 180 m altitude, flew level for 4 min, then climbed back through 500 m altitude at 0830 local time (1230 UT). The second pollution peak was encountered 15 km northeast of the first pollution peak. We analyze these two polluted air masses separately because the prevailing northwesterly wind direction (see Figure 5) could not have similarly influenced the two sampling locations.

during COBRA-NA. During the three flight legs from Edmonton, Alberta, to Mont Joli, Quebec, in late May (Figure 1), 20–25% of our CO and CHCl₃ measurements in the free troposphere (2 to 8.4 km altitude) were >200 ppb and >13 ppt, respectively, compared to clean air background mixing ratios of ~100 ppb CO and ~11 ppt CHCl₃. These enhancements were caused by hundreds of forest fires burning in Asia that generated vast smoke plumes across Canada during late May [Nedelec et al., 2005]. Air masses with high CO (>300 ppb) and high CHCl₃ (>13.5 ppt) were also sampled on 23 June, south of Chibougamau, Quebec, in a region where several large forest fires were burning.

[21] Evidence that biomass fires emit at least two of the trace gases analyzed in this study makes it imperative that their influences are removed before their anthropogenic emissions are determined. This is especially important for CO, which serves as the reference pollutant for emission ratio calculations. Scatterplots constructed from the entire data sets for CO, SF₆, and CHCl₃ (Figure 3) clearly show different correlations for air affected by biomass fire emissions and those influenced by anthropogenic sources. Though biomass fires are ignited by natural phenomena (e.g., lightning) and humans, in this work they are regarded as nonanthropogenic sources because they are typically not collocated with anthropogenic halocarbon sources. Data identified as significantly influenced by biomass fire emissions in the correlation plots (Figure 3, gray markers) were not used in our subsequent determinations of anthropogenic emissions.

[22] From the COBRA-NA data set we identified a total of 55 polluted air masses that were significantly influenced by anthropogenic sources but not biomass fires. Data for

three of these were discarded by our requirement that ≥ 3 concurrent measurements of CO, SF₆, CHCl₃, and each of the six restricted halocarbons were made within the air mass. Seven of the remaining 52 polluted air masses did not meet the requirements of the STILT model (see section 2.4), leaving 45 polluted air masses to be characterized (Table 2). These air masses were sampled in many different regions of the United States and Canada (Figure 1).

[23] Emission ratios for each restricted halocarbon were independently determined for the 45 polluted air masses by plotting mixing ratios of the gas of interest against the CO mixing ratios measured concurrently within the air mass, then linearly fitting the data (Figure 4). We also analyzed SF₆ and CHCl₃ data in this manner, as our intention is to estimate emissions of these nonregulated gases for comparison to other estimates. The methodology assumes a linear relationship between emissions of the gas of interest and CO, the slope of the linear relationship being the emission ratio.

[24] Uncertainties in emission ratios, calculated at the 95% level of confidence, incorporate individual measurement uncertainties and the goodness of fit of the regression lines. We did not attempt to correct emission ratios for the $\leq 10\%$ losses of the shorter-lived gases CO and CHCl₃ ($\tau \approx$

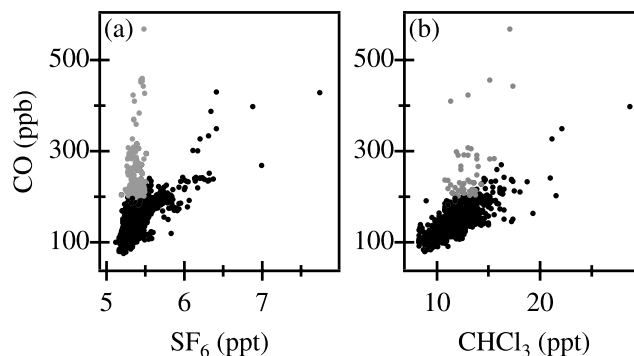


Figure 3. Correlation plots for (a) CO and SF₆ and (b) CO and CHCl₃ are used to identify air masses significantly influenced by biomass fire emissions. In Figure 3a, the upper branch (gray markers) shows elevated CO mixing ratios (>200 ppb) without notable enhancements in SF₆ mixing ratios (<5.5 ppt), indicative of influences by biomass fire emissions (see section 2.3). The SF₆ mixing ratio limit for the upper branch was calculated as the mean plus 2 standard deviations (2σ) of all SF₆ data. With this SF₆ limit applied, the CO mixing ratio limit was determined visually where the two correlation branches start to diverge at ~200 ppb CO. The lower branch (black markers) depicts mutual increases in CO and SF₆, evidence of industrial emissions [Bakwin et al., 1997]. In Figure 3b, gray markers portray measurements of CHCl₃ that were made concurrently with the biomass fire-influenced measurements of CO and SF₆ in Figure 3a. The gray markers form the biomass fire emissions (upper) branch of the correlation plot, with the industrial branch (black) below. Increases in CHCl₃ mixing ratios in the upper branch result from this gas being emitted by biomass fires [Lobert et al., 1999]. More gray markers appear in Figure 3a than in Figure 3b because the measurement rate for SF₆ was twice that of CHCl₃ (see Table 1).

Table 2. Polluted Air Masses Sampled and Their Associated Footprint-Weighted CO Fluxes

Date	Time, ^a UT	Latitude, °N	Longitude, °W	Altitude, ^b masl	CO Flux, μmol km ⁻² s ⁻¹
23 May 2003	1938:52	39.75	106.65	771	1717
23 May 2003	2006:15	39.55	105.26	1829	5557
25 May 2003	1654:10	40.44	107.42	331	2420
25 May 2003	1714:22	39.81	106.81	1214	2350
25 May 2003	1826:05	40.09	105.37	1819	2573
26 May 2003	1750:19	41.56	108.93	215	4439
26 May 2003	1841:05	42.39	113.66	2751	14,509
26 May 2003	2120:32	42.35	120.41	741	1808
26 May 2003	2152:17	42.41	122.49	1679	3436
28 May 2003	1959:14	41.18	124.17	889	2798
29 May 2003	1804:10	44.46	124.08	1285	457
29 May 2003	1830:04	46.07	123.89	829	1225
29 May 2003	2257:54	53.03	114.37	1371	2848
30 May 2003	0032:19	48.59	81.68	1569	3139
31 May 2003	1840:13	48.49	69.41	2052	1411
31 May 2003	2209:59	43.95	66.21	520	14,410
31 May 2003	2301:51	42.64	70.27	3353	9392
3 June 2003	2042:49	43.69	64.21	6642	4484
3 June 2003	2147:16	43.13	70.23	1535	4219
6 June 2003	1157:59	42.53	72.24	446	21,172
6 June 2003	1223:31	42.75	72.12	341	15,227
6 June 2003	1320:23	43.49	73.60	490	9794
6 June 2003	1358:32	43.14	70.94	464	11,203
11 June 2003	1821:16	41.23	74.43	907	12,852
11 June 2003	1939:00	39.48	76.40	793	11,918
12 June 2003	2008:19	42.14	97.02	9190	5984
14 June 2003	2014:10	30.21	97.59	616	4063
14 June 2003	0011:48	39.16	104.15	1858	19,684
16 June 2003	1618:53	36.41	97.94	7581	5169
16 June 2003	1648:44	36.35	97.10	1226	12,854
16 June 2003	2053:38	37.39	96.19	1848	9403
16 June 2003	2113:47	37.15	96.85	826	9000
16 June 2003	2133:23	36.61	97.48	1483	13,085
16 June 2003	2204:22	36.71	99.33	2136	9380
16 June 2003	2304:57	39.44	104.31	912	8676
18 June 2003	1851:50	42.21	120.30	868	4764
19 June 2003	2212:39	50.70	120.60	461	781
21 June 2003	2256:32	49.87	81.56	1385	3987
25 June 2003	1300:27	45.88	70.63	392	13,723
25 June 2003	1324:54	45.60	69.80	1266	5373
25 June 2003	1848:45	45.13	68.70	873	9537
25 June 2003	1920:45	45.52	68.59	709	6239
25 June 2003	2010:35	43.28	70.70	2299	10,476
27 June 2003	1440:18	39.40	76.35	1027	18,911
27 June 2003	1807:14	39.67	82.86	698	19,276

^aUniversal times (UT) are Eastern Daylight Time plus 4 hours.

^bAltitudes are given in masl, meters above sea level.

1 and 4 months in summer) during the 1–3 day transits of air masses from source regions to the measurement locations, nor for the potential source of CO from anthropogenic NMHC oxidation during transit. Such corrections would be small compared to the 52% mean uncertainty of the CO flux estimates used to calculate emissions (see section 2.4).

[25] Though sampling directly downwind of large population centers would have undoubtedly led to larger measured increases in mixing ratios, this is no guarantee of reduced uncertainties in the calculated emission ratios. The goodness of fit of each regression line depicts how well emissions of the two gases correspond in space and time. Near-field sampling may suffer from sources of the two gases being noncollocated or their emissions having different temporal patterns, resulting in poorly correlated mixing ratio increases. Sampling at greater distances can reduce

these potential spatiotemporal differences at the cost of smaller mixing ratio increases.

2.4. Determination of Footprints and Footprint-Weighted Fluxes

[26] The geophysical connection between source emission rates and emission ratios measured at a downwind location is atmospheric transport. During transport, an air mass may be exposed to any number of sources and sinks, each of which may or may not significantly perturb the composition of the air mass before it reaches the measurement location. The accuracy of an emission rate deduced from an emission ratio is largely dictated by how accurately the transport between source regions and the measurement location (receptor) is represented.

[27] We employed the Stochastic Time-Inverted Lagrangian Transport (STILT) model [Lin *et al.*, 2003; Gerbig *et al.*, 2003] to describe a 15-day transport history for each of the 52 polluted air masses identified in the COBRA-NA data. The model, driven by 80 km × 80 km resolution meteorological data from the Eta data assimilation system (EDAS), simulates transport by following the evolution of an ensemble of particles (representing air parcels of equal mass) backward in time from the receptor to source regions. EDAS data are derived from National Center for Environmental Prediction wind fields and archived by the NOAA Air Resources Laboratory. STILT interpolates these observation-based meteorological fields to the subgrid-scale location of each particle because transport in the near field, where upstream sources and sinks have strong influences on observations, often takes place on scales not resolved by typical grid sizes in transport models. STILT provides the capability to represent near-field influences on tracer concentrations at high spatiotemporal resolution, such as constraining regional-scale CO₂ fluxes from aircraft-based observations of CO₂ over the United States [Gerbig *et al.*, 2003].

[28] STILT maps the spatiotemporal distribution of potential source influences on the composition of the receptor air mass as a footprint. The footprint is deduced solely from transport representations, without any knowledge of sources in the upwind sector. Footprints are composed of elements gridded at a maximum spatial resolution of 1/6° latitude × 1/4° longitude. Resolution is reduced as the simulated particles travel backward in time and disperse over a wider region [Gerbig *et al.*, 2003]. The model successfully mapped footprints for 45 of the 52 COBRA-NA receptors including the polluted air mass discussed in both Figures 2 and 4 (Figure 5). Footprints for six polluted air masses could not be determined because the model found no significant connection between their free tropospheric receptors and the planetary boundary layer where the sources are located. This likely resulted from the lack of convective storm representation in the EDAS. One receptor north of 55°N latitude could not be studied because the EDAS meteorological data do not extend that far north. Typical transit times of particles from receptors to footprint elements were 1–3 days. The areas of the 45 footprints were generally 10³ to 10⁴ km², considerably larger than footprints associated with surface receptors because the COBRA-NA receptors were >200 m above the ground.

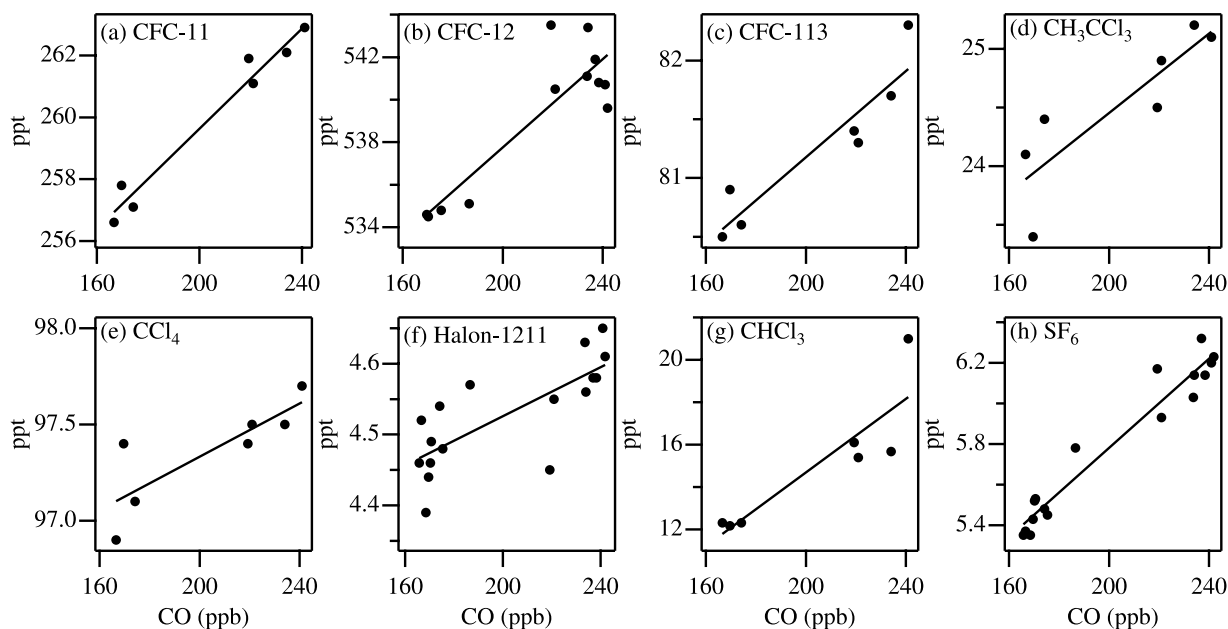


Figure 4. Mixing ratios of (a–f) the six restricted halocarbons, (g) CHCl₃, and (h) SF₆ are plotted against CO mixing ratios measured coincidentally in the second polluted air mass sampled during the morning flight of 6 June 2003 (see Figure 2). The data in each panel were fit using a linear orthogonal distance regression algorithm [Press *et al.*, 1992] that accounts for uncertainties in both the x and y variables. Prior to fitting, approximately 3 min of nonpollution data, obtained just before and after the polluted air mass was sampled, were added to each panel to help anchor the lower ends of fit lines. The slope of a fit line is the emission ratio of that gas relative to CO for that specific air mass. Uncertainties in emission ratios were calculated at the 95% level of confidence.

[29] An important outcome of the STILT footprint computations is that the composite of footprints for all 45 COBRA-NA receptors (Figure 6) spans a wide geographical range of the United States and Canada and extends over many of the large population centers in each country. Of the 12 most populous metropolitan areas in the United States, only Miami–Fort Lauderdale (southern Florida) lies outside the composite of footprints (Figure 6). This footprint coverage is greatly beneficial to our objective of estimating halocarbon emission rates at large spatial scales, especially since sources of restricted halocarbons in the United States and Canada are no longer expected to be ubiquitous. Though only 7 receptors were located in Canada (Figure 1), an additional 9 footprints for receptors in the northeastern United States include important elements north of the border, predominantly in Ontario and Quebec (Figure 6) where 62% of Canadians reside.

[30] One advantage of calculating emission ratios relative to CO is the availability of inventory-based CO emission estimates at spatial scales similar to the resolution of the STILT footprint elements. Gerbig *et al.* [2003] produced a spatial grid of anthropogenic CO fluxes by combining the 1990 National Acid Protection Assessment Program (NAPAP) CO emission estimates ($1/6^\circ$ latitude \times $1/4^\circ$ longitude resolution) for the northeastern United States [Environmental Protection Agency (EPA), 1993] with $1^\circ \times 1^\circ$ CO emissions calculated from Global Emissions Inventory Activity (GEIA) emission estimates for NO_x [Benkovitz *et al.*, 1996]. The latter estimates derive from

the tight linear correlation between GEIA NO_x emission estimates and the NAPAP CO emission estimates in their area of overlap [Gerbig *et al.*, 2003]. We mapped these CO emission estimates onto each COBRA-NA footprint, adjusting the fluxes for the time of day and day of week [Ebel *et al.*, 1997] associated with each footprint element, to generate a footprint-weighted CO flux estimate for each footprint (Table 2). These footprint-weighted fluxes (hereinafter referred to as flux estimates) ranged from 457 to 21,200 $\mu\text{mol CO km}^{-2} \text{s}^{-1}$ (404 to 18,700 $\text{kg CO km}^{-2} \text{yr}^{-1}$) and averaged 7900 $\mu\text{mol CO km}^{-2} \text{s}^{-1}$ (7000 $\text{kg CO km}^{-2} \text{yr}^{-1}$).

[31] Uncertainties in our CO flux estimates propagated from errors in the transport representations that define the footprints, and from uncertainties in the inventory-based CO emission estimates. These two sources of error were difficult to assess independently, so we evaluated their combined uncertainties by comparing measured and model-derived CO mixing ratios at all 45 receptors. The model calculated background CO mixing ratios from a latitude- and altitude-dependent boundary condition over the Pacific [Gerbig *et al.*, 2003], incorporated CO losses during transport by OH fields simulated by a global chemical transport model, and derived CO fluxes by mapping CO emission fields onto the STILT-derived footprints. The root-mean-square difference between measured and model-derived CO mixing ratios at all 45 receptors (± 41 ppb) is a logical measure of the combined uncertainties of CO emission fields and STILT transport representations. However, it is also inclusive of a ± 22 ppb average error in the simulated background CO mixing ratios [Gerbig *et al.*, 2003], which

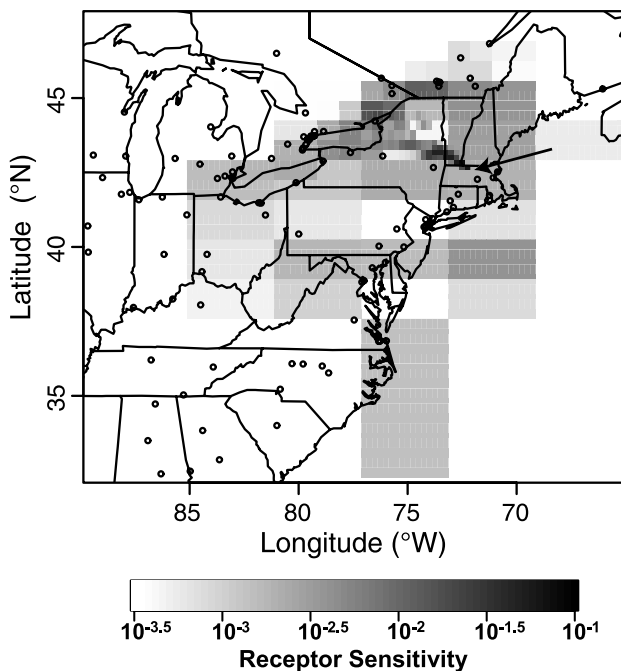


Figure 5. Footprint calculated by the STILT model for the same polluted air mass discussed in both Figures 2 and 4. The sampling location (receptor) in northern central Massachusetts is indicated by the tip of the arrowhead. The sensitivity of the receptor to each footprint element (grid cell) is expressed in units of mixing ratio enhancement (ppm) at the receptor per unit surface flux of an inert tracer ($\mu\text{mol m}^{-2} \text{s}^{-1}$) released uniformly within the footprint element. These sensitivities are based solely on transport representations by STILT and hold no information about actual surface fluxes. Footprint element resolution is reduced as STILT moves backward in time and simulated particles spread out [Gerbig *et al.*, 2003]. A logarithmic scale is required to illustrate the full range of receptor sensitivities, with darker shades indicating greater sensitivities. Small open circles show the locations of cities with populations greater than 100,000.

should be excluded from our assessment of CO flux uncertainties. Removing (in quadrature) this ± 22 ppb error from the ± 41 ppb mean uncertainty of model-derived CO mixing ratios at receptors leaves a ± 35 ppb mean uncertainty in simulated CO enhancements. Relative to the mean CO mixing ratio enhancement measured at receptors (67 ppb), the relative error in our CO flux estimates is estimated to be $\pm 52\%$.

[32] For each footprint, the flux of trace gas X (F_X) was computed as the product of the CO flux (F_{CO}) and the emission ratio ($\Delta X/\Delta \text{CO}$) measured at the associated receptor,

$$F_X = F_{\text{CO}} \bullet \Delta X/\Delta \text{CO}. \quad (1)$$

Fluxes of the six restricted halocarbons, SF_6 , and CHCl_3 were 4–6 orders of magnitude weaker than CO fluxes, with mean fluxes ranging from $10 \text{ nmol km}^{-2} \text{ s}^{-1}$ ($0.05 \text{ kg km}^{-2} \text{ yr}^{-1}$) for CCl_4 to $620 \text{ nmol km}^{-2} \text{ s}^{-1}$ ($2.4 \text{ kg km}^{-2} \text{ yr}^{-1}$) for CFC-12. Uncertainties in halocarbon

fluxes were propagated, in quadrature, from the uncertainties in emission ratios and the 52% mean error in CO fluxes. The fact that some halocarbon emission ratios (slopes) were negative translates to negative fluxes, which are physically impossible for these long-lived halocarbons. Negative emission ratios and fluxes were predominantly associated with polluted air masses having weak or no halocarbon mixing ratio enhancements. Most negative flux values carry large enough uncertainties that they are not statistically different from zero.

2.5. Estimates of Per Capita Emission Rates

[33] The extensive geographical coverage of the 45 COBRA-NA footprints (Figure 6) is an enticement to estimate halocarbon emission rates in the United States and Canada from simple averages of their fluxes or emission ratios to CO. However, we consider these approaches risky because so little is known about the contemporary spatial distributions of halocarbon sources in these two countries. Instead we rely on the expectation of quantitative relationships between population and the emissions of anthropogenic halocarbons. Population data were mapped onto the footprints in much the same way as the inventory-based CO emission estimates. For the United States we scaled county-by-county population data from the 2000 census to 2003 in accordance with annual increases in the national population between 1995 and 2000. Canadian population data for 1990, available at 1° latitude \times 1° longitude resolution, were scaled to 2003 on the basis of national population growth between 1990 and 2004. The two sets of 2003 population data were regridded to the CO emission inven-

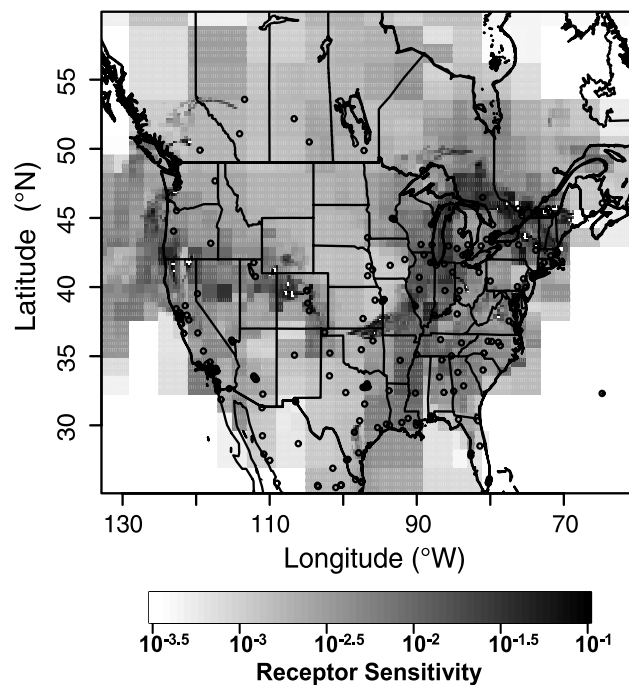


Figure 6. Composite of footprints for all 45 receptors (not shown) that appear in Figure 1. Small open circles show the locations of cities with populations greater than 100,000. Together, the footprints include most of the large population centers in the continental United States and southern Canada.

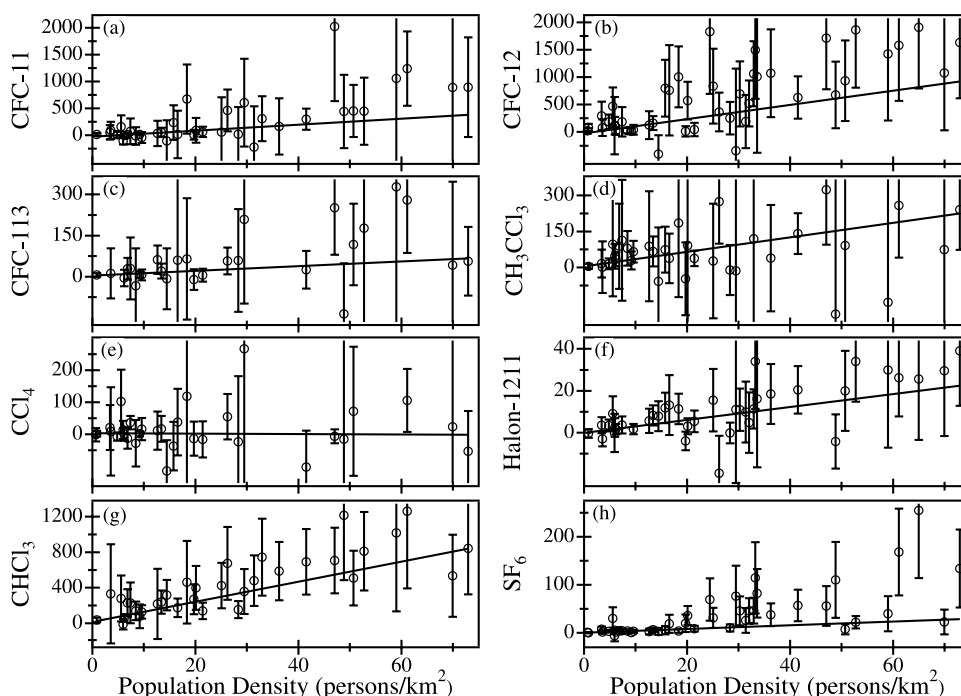


Figure 7. Fluxes of (a–f) the six restricted halocarbons, (g) CHCl_3 , and (h) SF_6 , in units of $\text{nmol km}^{-2} \text{s}^{-1}$, are plotted against the corresponding footprint-weighted population densities. Error bars represent flux uncertainties (at the 95% level of confidence), which propagated from uncertainties in emission ratios and footprint-weighted CO fluxes (see section 2.5). The data were fit with a linear orthogonal distance regression assuming a population density uncertainty of 10%. The slopes of fit lines are per capita emission rates ($\text{nmol person}^{-1} \text{s}^{-1}$) for the continental United States and Canada.

tory grids used in this work, then mapped onto COBRA-NA footprints to produce footprint-weighted population densities (hereinafter referred to as population densities).

[34] Fluxes of the six restricted halocarbons, SF_6 , and CHCl_3 in each of the 45 COBRA-NA footprints were plotted against their associated population densities and fit with a linear orthogonal distance regression (Figure 7). Population densities were assigned uncertainties of 10% estimated from errors in census data, temporal extrapolations of these data, and the regriding process. Negative flux values and their uncertainties were included because they carry important information about footprints with weak or no halocarbon fluxes. The slopes of fit lines, representing best estimates of per capita emission rates ($\text{nmol person}^{-1} \text{s}^{-1}$) were significantly different from zero at the 95% confidence level for SF_6 , CHCl_3 , and each of the six restricted halocarbons except CCl_4 (Table 3), for which there was some evidence of emissions (Figure 7) but no statistically significant linear relationship with population. All fit lines pass very near to the origins, supporting the expectation that anthropogenic emissions should not emanate from footprints with zero population.

[35] We also calculated the per capita CO emission rate as a test of our methods for determining the per capita emissions of restricted halocarbons (Table 3). The calculation for CO uses the same methods and data involved in determining halocarbon emissions except for the measured halocarbon emission ratios. Uncertainties in the model-derived CO fluxes and population densities for the 45 footprints were incorporated into a 95% confidence interval for the estimated per capita CO emission rate.

[36] Footprint population densities in this study spanned a range of 0.6 to 73 persons km^{-2} . This range encompasses the average population densities of the United States (30.7) and Canada (3.2), but does not approach the high population densities of the 20 most populous cities in the United States (mean = 2760 persons km^{-2}). The COBRA-NA receptors were undoubtedly influenced by large cities (Figure 6), but at spatial scales that incorporated footprint elements from both urban and rural areas, as revealed by footprints that are considerably larger than the areas of densely inhabited cities.

2.6. Estimates of Annual Emissions

[37] Given the extensive spatial coverage of COBRA-NA footprints (Figure 6) and the statistical significance of per capita emission rates (Figure 7), we estimated halocarbon emission rates for the continental United States and Canada together (CONUS + CAN) for the period 23 May to 28 June 2003. Spatial coverage of the COBRA-NA footprints in the far north of Canada was very limited, but the footprint elements within Canada indicate strong influences from large population centers in Ontario and Quebec (see section 2.4). No attempt was made to differentiate between emissions in the CONUS and Canada because 16 of the 45 footprints had important elements on both sides of the border. Population estimates of 288.9 million (CONUS) and 31.7 million (CAN) in 2003 comprising a total population of 320.6 million were used to scale the per capita emission rates into emission rates for the CONUS + CAN. On the basis of population alone our emission estimates are composed of 90% CONUS emissions and 10% Canadian emissions.

Table 3. Per Capita Emission Estimates for Regulated Halocarbons, CHCl₃, SF₆, and CO^a

Chemical	This Work (2003) ^b	<i>Li et al.</i> [2005] for Year 2002 ^c	<i>Li et al.</i> [2005] (Year) ^d	Other Studies (Year)	<i>Barnes et al.</i> [2003] for Year 1998 ^e
CFC-11	0.024 ± 0.009	0.016	0.027 (1999–2002)	0.054 ^f (2002)	0.050
CFC-12	0.049 ± 0.014	0.040	0.060 (1999–2002)	0.099 ^f (2002)	0.113
CFC-113	0.005 ± 0.003	0.001	0.002 (1999–2002)	<0.0002 ^f (2002)	0.014
CH ₃ CCl ₃	0.013 ± 0.004	0.006	0.008 (2001–2002)	<0.0002 ^f (2002), 0.013 ^g (2002)	0.044
CCl ₄	–0.0003 ± 0.0021			0.087 ^f (2002)	
Halon-1211	0.0016 ± 0.0005			<0.0002 ^f (2002), 0.004 ^h (2003)	0.0022
CHCl ₃	0.043 ± 0.013	0.066		0.06 ± 0.02 ⁱ (1995)	
SF ₆	0.0018 ± 0.0007			0.008 ± 0.002 ^j (1995), 0.0028 ^j (2003)	
CO	0.22 ± 0.05			0.28 ^k (2003), 0.25 ^k (2000)	

^aAll estimates are in kg person^{–1} yr^{–1} except for CO, which is given in Mg (1 × 10⁶ g) person^{–1} yr^{–1}.

^bFor the continental United States and Canada.

^cCalculated from 2002 per capita emission estimates for California and for Oregon and Washington [*Li et al.*, 2005]. Table values are population-weighted West Coast averages for 2002 using populations of 35.1 million (California) and 9.59 million (Oregon and Washington). The estimate for CHCl₃ is the population-weighted average of annual mean per capita emission estimates for 1996–2002 [*Li et al.*, 2005].

^dEstimates for CFC-11, CFC-12, and CFC-113 were calculated from 4-year mean U.S. emission estimates for 1999–2002 and for CH₃CCl₃ from a 2001–2002 mean U.S. emission estimate [*Li et al.*, 2005]. See section 3.1 for more details.

^eThe 1998 estimates are for the New York City–Washington, D. C., corridor [*Barnes et al.*, 2003].

^fCalculated from 2002 inventory-based U.S. emission estimates of 15.4 Gg CFC-11, 28.6 Gg CFC-12, and 25 Gg for CCl₄ [*EPA*, 2004]. Values of <0.0002 kg person^{–1} yr^{–1} for CFC-113, CH₃CCl₃, and Halon-1211 result from 2002 U.S. emission estimates of <0.05 Gg yr^{–1} for each [*EPA*, 2004].

^gCalculated from the 2002 U.S. estimate of 3.7 Gg CH₃CCl₃ [*Millet and Goldstein*, 2004].

^hCalculated from a 2003 inventory-based emission estimate of 1.18 Gg Halon-1211 for the United States and Canada [*UNEP*, 2003a].

ⁱCalculated from 1995 emission estimates of 17 ± 6 Gg CHCl₃ and 2.4 ± 0.5 Gg SF₆ for the United States and Canada [*Bakwin et al.*, 1997].

^jCalculated from 2003 inventory-based U.S. emission estimates of 0.81 Gg SF₆ and 80,600 Gg CO [*EPA*, 2005]. Estimates for restricted halocarbon emissions in 2003 were not published as part of this most recent report.

^kCalculated from a 2000 inventory-based emission estimate of 80,200 Gg CO [*Olivier et al.*, 2005] for the United States and Canada. Excludes emissions from agricultural and forest fires.

[38] The estimation of halocarbon emissions in the CONUS + CAN during all of 2003 required temporal scaling of emission rates descriptive of the ~1 month duration of our study to the entire year. The relatively short duration of this measurement campaign could introduce biases in our emission estimates if we do not consider the possibility of seasonally dependent halocarbon emission rates. Seasonal influences on halocarbon emission rates include the higher demand for air conditioning and refrigeration during warmer months.

[39] We assess the need for seasonal adjustments to our emission rates by examining reported seasonal variations in the emission ratios of CFC-11, CFC-12, CH₃CCl₃, and Halon-1211 to CO in the northeastern United States during 1996–1998 [*Barnes et al.*, 2003]. In the northeast United States, the highest and lowest emission ratios of these four halocarbons were observed in summer and winter, respectively, with spring and fall emission ratios closer to annual mean values. No seasonality in ΔCFC-113/ΔCO values was observed. Since the COBRA-NA study period included the last month of spring and first week of summer, we averaged the *Barnes et al.* [2003] spring and summer emission ratios for each year and divided by the mean emission ratio for that year. Three-year averages of these quotients were 1.09 ± 0.11 for CFC-11, 1.13 ± 0.15 for CFC-12, 0.99 ± 0.18 for CH₃CCl₃, and 1.06 ± 0.16 for Halon-1211. Since these mean values are not statistically different from unity, our CONUS + CAN emissions for 2003 were determined by linearly scaling the COBRA-NA emission rates to the entire year (Table 4).

3. Results and Discussion

3.1. Per Capita Emissions

[40] The per capita emission rate for CO derived in this study, 220 ± 50 kg person^{–1} yr^{–1} (Table 3), provides a

value for comparison to other estimates and a test of our calculation methods. Our value is in good agreement with independent inventory-based estimates of anthropogenic CO emissions in the United States [*EPA*, 2005] and in the United States and Canada [*Olivier et al.*, 2005]. For the purpose of comparison we excluded CO emissions from agricultural and other biomass fires that were part of the inventory-based estimates. The concordance between these three estimates supports our method of calculating halocarbon emissions using the COBRA-NA data and the STILT model.

[41] Our per capita emission estimates for restricted halocarbons CFC-11, CFC-12, CFC-113, CH₃CCl₃, and Halon-1211 (Table 3) are 27% to 70% lower than those reported for the northeastern United States in 1998 [*Barnes et al.*, 2003]. The decreases indicate that emission reductions during 1998–2003 averaged >10% yr^{–1} for each of

Table 4. Anthropogenic Emissions of Restricted Halocarbons, CHCl₃, and SF₆^a

Chemical	CONUS and Canada (2003)	Global (Year)
CFC-11	8 ± 3	71 (2003) ^b
CFC-12	16 ± 4	92 (2003) ^b
CFC-113	2 ± 1	4 (2003) ^b
CH ₃ CCl ₃	4 ± 1	39 (2003) ^b
CCl ₄	–0.1 ± 0.7	64 (2003) ^b
Halon-1211	0.5 ± 0.2	7 (2003) ^b
CHCl ₃	14 ± 4	70 (1990) ^c
SF ₆	0.6 ± 0.2	5.9 ± 0.2 (1996) ^d

^aAll emission estimates are in Gg yr^{–1}.

^bEstimates for 2003 are from the halocarbon emission scenario Ab [*Montzka and Fraser*, 2003], which incorporated current data for production trends, emissions of new production, bank sizes, and bank release rates.

^cEstimate of anthropogenic emissions from *Aucott et al.* [1999].

^dFrom *Geller et al.* [1997].

these halocarbons except for Halon-1211 ($5\% \text{ yr}^{-1}$), which is predominantly banked in hermetic fire extinguishing systems. These two independent sets of halocarbon emission estimates demonstrate the efficacy of production bans imposed by the Montreal Protocol to reduce emissions of ozone-depleting gases in developed countries.

[42] Our 2003 per capita emission estimates for CFC-11, CFC-12, CFC-113, and CH_3CCl_3 (Table 3) are all $>20\%$ higher than 2002 estimates for the U.S. West Coast [Li *et al.*, 2005]. The 2002 estimates were based on routine measurements at Trinidad Head, California (41°N , 124°W) that reportedly captured emission signals from only California, Oregon, and Washington. For nonregulated CHCl_3 , the 1996–2002 average of per capita emissions from the West Coast states [Li *et al.*, 2005] is 50% greater than our CONUS + CAN estimate for 2003 (Table 3). These differences may stem from locational biases in emission rates, as indicated by 30–120% disparities between U.S. West Coast and northeastern United States per capita emission rates for 1996–1998 [Li *et al.*, 2005; Barnes *et al.*, 2003], as well as from the very dissimilar methods used to calculate per capita emission rates here and in the Li *et al.* [2005] study.

[43] The COBRA-NA per capita emission estimates are also compared (Table 3) against the Li *et al.* [2005] emission estimates for the entire United States. These authors combined their West Coast per capita emission rates with temporal extrapolations of the 1996–1998 northeastern U.S. estimates of Barnes *et al.* [2003] to formulate U.S. emission estimates. Unfortunately, the only U.S. emission estimates presented by Li *et al.* [2005] for CFC-11, CFC-12, and CFC-113 are 4-year averages for 1999–2002 (Table 3). Their 4-year average values for these three halocarbons are not statistically different from the COBRA-NA results for 2003, but the general downward trends in U.S. emissions of restricted halocarbons since 1996 [Barnes *et al.*, 2003; Li *et al.*, 2005] suggest that their 1999–2002 mean values should be considerably higher than our 2003 estimates. It is beyond the scope of this work to interpret the similarity of the 1999–2002 mean and 2003 per capita emission estimates for CFC-11, CFC-12, and CFC-113 as agreement or disagreement between these independently derived estimates. However, there is a statistically significant difference between our 2003 per capita emission estimate for CH_3CCl_3 ($0.013 \pm 0.004 \text{ kg person}^{-1} \text{ yr}^{-1}$) and the Li *et al.* [2005] mean value for 2001–2002 ($0.008 \text{ kg person}^{-1} \text{ yr}^{-1}$). Our value for CH_3CCl_3 is in excellent agreement with an independent estimate of U.S. CH_3CCl_3 emissions in 2002 [Millet and Goldstein, 2004] that was based on several 1–2 month sets of ground-based measurements at three different sites during spring, summer, and winter.

[44] It is also of interest to compare our per capita emission estimates with inventory-based estimates of halocarbon emissions (Table 3) published annually by the U.S. Environmental Protection Agency (EPA) [e.g., EPA, 2003] (see yosemite.epa.gov/oar/globalwarming.nsf/content/ResourceCenterPublicationsGHGEmissions.html). Important revisions were made in 2003–2004 to the EPA's vintaging model that computes annual emissions in the United States from national usage and leak rate data (D. Godwin, personal communication, 2004). These model adjustments invoked large changes in the U.S. halocarbon

emissions already reported by the EPA for 2001 and previous years. For example, relative to the 2001 EPA emission estimates published in 2003 [EPA, 2003], the revised emission estimates for 2001 published in the 2004 report [EPA, 2004] are 30% lower for CFC-11, $>95\%$ lower for Halon-1211, 65% higher for CFC-12, and a factor of >500 higher for CCl_4 . The EPA's estimates for 2002 [EPA, 2004] depict per capita emissions of CFC-11 and CFC-12 that are more than twice the 2003 COBRA-NA estimates, while our estimates for CFC-113, CH_3CCl_3 , and Halon-1211 are higher by at least an order of magnitude (Table 3). In contrast, our Halon-1211 value is only 40% of a different inventory-based emission estimate for the United States and Canada during 2003 [UNEP, 2003a]. By far, the greatest disagreement in per capita emission estimates (Table 3) is between our CCl_4 value of $-0.3 \pm 2.1 \text{ g person}^{-1} \text{ yr}^{-1}$ and the EPA [2004] value of $87 \text{ g person}^{-1} \text{ yr}^{-1}$ for 2002. Though we did measure some weakly enhanced CCl_4 mixing ratios during COBRA-NA, it is difficult to comprehend how the strong emissions of this halocarbon implied by the EPA estimate are not revealed by our measurements. Note that the EPA did not include inventory-based emission estimates of restricted halocarbons for 2003 or former years in its most recent report [EPA, 2005].

[45] COBRA-NA per capita emission estimates of CHCl_3 and SF_6 are compared to 1995 estimates for the United States and Canada (Table 3) that were based on routine ground-based measurements in eastern North Carolina, United States [Bakwin *et al.*, 1997]. These authors scaled up regional relationships between the mixing ratios of CHCl_3 , SF_6 , and C_2Cl_4 using an inventory-based 1995 C_2Cl_4 emission estimate for the United States and Canada. Our estimates of anthropogenic per capita CHCl_3 and SF_6 emissions in 2003 are 28% lower and 78% lower, respectively, than the 1995 estimates of Bakwin *et al.* [1997]. It is clear that the slope of the fit line for SF_6 (Figure 7h), and therefore our per capita emission estimate for this gas, is constrained by the smaller uncertainties (i.e., greater weights in the fitting algorithm) of the lower SF_6 flux estimates and not by the higher flux estimates with larger uncertainties. The Bakwin *et al.* [1997] estimate for SF_6 may also be higher because of a sample location bias or a decrease in American and Canadian emissions between 1995 and 2003. Though the relatively constant global SF_6 growth rate of $\sim 0.2 \text{ ppt yr}^{-1}$ between 1995 and 2003 [Geller *et al.*, 1997; Thompson *et al.*, 2004] attests to stable global emissions during this period, it does not rule out a significant decrease in American and Canadian SF_6 emissions as developing nations enlarge their capacities for electrical power distribution. In fact, the U.S. Department of Energy reported a 36% decrease in SF_6 emissions in the United States between 1995 and 2003 [Department of Energy, 2004] (see www.eia.doe.gov/oiaf/1605/gg04rpt/index.html) based on annual SF_6 emission estimates from the EPA [2005]. The EPA [2005] estimate for 2003 SF_6 emissions in the United States is 50% greater than our value (Table 3).

3.2. Global Significance of Emissions From the Continental United States and Canada

[46] Estimates of contemporary global emissions of restricted halocarbons are required to ascertain whether emis-

sions in the United States and Canada are still of global significance. We utilize the global emission estimates from the baseline emission scenario Ab [Montzka and Fraser, 2003] that assumed global compliance with the Montreal Protocol production and consumption timelines for developed and developing countries (Table 4). The scenario collectively employed historical records of production, application-based release functions, and measured changes in the atmospheric burdens of restricted halocarbons to produce an emission record through the year 2000, then from 2001 onward utilized contemporary trends in halocarbon production, consumption, and release functions, along with assessments of the sizes and release rates of modern ODS banks to predict global emissions [Montzka and Fraser, 2003].

[47] Our emission estimates provide compelling evidence that American and Canadian emissions of five of the six restricted halocarbons studied here are still globally significant. Relative to the Montzka and Fraser [2003] global estimates for 2003, our CONUS + CAN emissions account for $11 \pm 4\%$ (CFC-11), $17 \pm 4\%$ (CFC-12), $40 \pm 30\%$ (CFC-113), $10 \pm 3\%$ (CH_3CCl_3), and $7 \pm 2\%$ (Halon-1211) of global emissions. In contrast, the upper end of our 95% confidence band for 2003 emissions of CCl_4 (0.6 Gg yr^{-1}) corresponds to only 1% of global CCl_4 emissions. Our CONUS + CAN emission estimates for CHCl_3 and SF_6 account for $20 \pm 5\%$ and $10 \pm 3\%$ of the global anthropogenic emissions estimated for 1990 and 1996, respectively (Table 4).

[48] Explicit reasons for the continued persistence of globally significant emissions of restricted halocarbons in the United States and Canada are not easily ascertained. However, at a minimum, we should be able to evaluate whether contemporary halocarbon emissions in these two countries emanate from banked or newly produced materials by examining national production and consumption figures reported to UNEP for 2002 and 2003 [UNEP, 2004, 2005]. Unfortunately, UNEP publishes only aggregated, ozone depletion potential (ODP)–weighted production and consumption figures for CFCs and halons, but the aggregated UNEP figures for CFCs (Annex A, Group 1) are dominated by the production and consumption of CFC-11, CFC-12, and CFC-113. The current ODP values employed by UNEP, relative to a CFC-11 ODP value of 1.0, are 1.0 for CFC-12, 0.8 for CFC-113, 0.1 for CH_3CCl_3 , 3.0 for Halon-1211, and 1.1 for CCl_4 [UNEP, 2002a].

[49] Note that the UNEP definition of production is the difference between annual manufacture for nonfeedstock use and any amount destroyed in the same year. Consumption is calculated as annual production plus imports minus exports. Equivalence between UNEP consumption figures and annual emissions cannot be assumed because this requires all materials produced and imported during a given year to be emitted in the same year. If annual consumption is greater than emissions, the unemitted portion is regarded as an addition to the bank. Annual emissions considerably greater than consumption figures imply that bank releases are responsible for the preponderance of emissions. These comparisons rely on assumed compliance with the Montreal Protocol such that there is no significant unreported production or consumption in the United States and Canada, including illicit importation.

[50] Here it is important to note again that developed countries like the United States were granted allowances to manufacture and consume small amounts of CFCs after 1995 for essential uses in medical devices such as metered-dose inhalers (MDIs), and to produce and export limited quantities of restricted halocarbons to developing countries. The 2-year sums (2002–2003) of CFC production and consumption figures reported by the United States were 1.1 ODP-Gg and 2.9 ODP-Gg, respectively [UNEP, 2004, 2005], revealing a mean net importation of $0.9 \text{ ODP-Gg CFCs yr}^{-1}$ during this period. Similar 2-year sums for CH_3CCl_3 production and consumption in the United States were both 0.004 ODP-Gg (0.04 Gg). Canada reported negligible production and consumption of CFCs and CH_3CCl_3 during both 2002 and 2003. The United States and Canada have both reported zero production and consumption of halons since 1994.

[51] With zero production and consumption of halons in the United States and Canada reported since 1994, the only plausible sources of Halon-1211 emission are releases of banked materials. For CFCs and CH_3CCl_3 , the combined United States and Canada consumption figures for 2002 and 2003 together represent only 12% and 1% of our 2003 CONUS+CAN emission estimates (Table 4) for CFCs ($25 \text{ ODP-Gg yr}^{-1}$) and CH_3CCl_3 ($0.4 \text{ ODP-Gg yr}^{-1}$), respectively. This implicates banks as the predominant emission sources of CFCs and CH_3CCl_3 in these two countries during 2003. The notion of modern banks of CFC-113 and CH_3CCl_3 , solvents once expected to be released to the atmosphere within a year of their production, is novel. The only way a significant fraction of the 2003 CONUS+CAN emissions of CFC-113 ($2 \pm 1 \text{ Gg}$) did not emanate from banks is if CFC-113 was the primary CFC consumed in the United States and Canada during 2002–2003. This is unlikely because CFC-11 and CFC-12, not CFC-113, are used in MDIs.

[52] A comparison of the COBRA-NA emission estimate for CCl_4 with UNEP CCl_4 production and consumption figures is of limited utility because UNEP does not include amounts manufactured for feedstock use, which is believed to be the major emission source for CCl_4 [Simmonds *et al.*, 1998]. Nonetheless, our finding of $-0.1 \pm 0.7 \text{ Gg CCl}_4$ emissions in 2003 supports the reported small (0.6 ODP-Gg) production of CFCs in the United States and Canada during that year. Interestingly, the United States reported CCl_4 production and consumption of 2.8 ODP-Gg (2.5 Gg) and 0.8 ODP-Gg (0.7 Gg) in 2001 after 5 years of near-zero production and large negative consumption [UNEP, 2002a, 2002b, 2003b], followed by negative production and consumption in both 2002 and 2003 [UNEP, 2004, 2005]. Whatever the reason for this sudden surge in CCl_4 production and consumption in 2001, it evidently did not result in large-scale CCl_4 emissions in the United States during mid-2003.

3.3. Persistence of Bank Releases and Their Consequences

[53] The persistence of globally significant bank releases of CFC-11, CFC-12, CFC-113, CH_3CCl_3 and Halon-1211 in the United States and Canada raises important questions about the sizes and release rates of modern global ODS banks. Indeed the United States and Canada produced

globally important amounts of these halocarbons until the early to middle 1990s, but is it reasonable to assert that these ODSs are still being released in globally significant quantities >7 years later? Residence times for CFC-11 and CFC-12 in blown foam products, refrigerators, and air conditioners, and for Halon-1211 in fire extinguishing systems may be several years to a decade or more [Fraser *et al.*, 1999; McCulloch *et al.*, 2001, 2003], but the solvents CFC-113 and CH₃CCl₃, and feedstock CCl₄ were generally regarded as nonbanked halocarbons emitted within a year of their manufacture [Fraser *et al.*, 1996; McCulloch and Midgley, 2001; Simmonds *et al.*, 1998]. Our observations of persistent American and Canadian emissions of CFC-113 and CH₃CCl₃ in 2003 suggest that their release functions have changed dramatically. It is clear that all five of these restricted halocarbons are being held for longer periods of time after manufacture and before release to the atmosphere, perhaps as a result of stockpiling or increased recycling.

[54] The implications of increased bank residence times for ozone-depleting halocarbons are twofold. First and foremost is the potential underestimation of the sizes of global ODS banks, and hence, future global emissions which would directly impact projections of stratospheric ozone recovery. Halocarbon emissions from banks around the globe may simply be stronger and perpetuate further into the future than anticipated, delaying ozone recovery. Second, release functions used in inventory-based global emission estimates may not accurately describe the modern evolution of banks. Functions that release banked chemicals too rapidly can quickly deplete banks, especially in the absence of new production, and lead to prematurely depleted banks and diminished emissions. This may be the case for an inventory-based global CFC-12 bank estimate of 60 Gg in 2000 [Montzka and Fraser, 2003] that implied the bank would be exhausted by 2002, a conclusion in stark contrast to a new equipment-based CFC-12 bank estimate of ~700 Gg in 2002 [IPCC/TEAP, 2005]. There are obvious difficulties in estimating the sizes of modern ODS banks and these contribute substantial uncertainty to scenarios of future halocarbon emissions, and in turn, projections of ozone recovery.

[55] Increased bank residence times and their potential impacts on inventory-based emission estimates may hold an important consequence for the CH₃CCl₃-based inference of a decreasing trend in the global abundance of the hydroxyl radical (OH) during the 1990s. Prinn *et al.* [2001] asserted that the diminishing abundance of CH₃CCl₃ in the atmosphere was not as rapid as expected from declining emissions and the well understood rate of CH₃CCl₃ removal by OH, hence the inference of a decreased global OH abundance. Their model employed inventory-based emission estimates [McCulloch and Midgley, 2001] that depicted global CH₃CCl₃ emissions peaking in 1990 then diminishing rapidly to <20 Gg yr⁻¹ by the year 2000. In comparison, halocarbon emission scenario Ab [Montzka and Fraser, 2003] estimated global CH₃CCl₃ emissions at 43 Gg yr⁻¹ in 2000, and Krol *et al.* [2003] determined that European CH₃CCl₃ emissions in 2000 were >20 Gg yr⁻¹ from aircraft-based measurements. Increasing the global CH₃CCl₃ emissions employed by Prinn *et al.* [2001] in accordance with these more recent global and European

emission estimates would negate or even reverse the inferred downward trend in OH abundance.

4. Summary of Results

[56] Estimates of the emissions of six restricted halocarbons in the continental United States and Canada during 2003 are presented (Table 4). The estimates are based on a geographically extensive set of halocarbon and CO measurements across the United States and Canada in May–June 2003, a gridded inventory of CO emissions in these two countries, and the STILT model, which quantitatively links polluted air masses to their upwind source regions. Our estimates reveal the continued global significance of American and Canadian emissions of CFC-11 (11 ± 4% of global), CFC-12 (17 ± 4%), CFC-113 (40 ± 30%), CH₃CCl₃ (10 ± 3%), and Halon-1211 (7 ± 2%) more than 7 years after their domestic production was banned by the Montreal Protocol. Our emission estimate for CCl₄ is not statistically different from zero, but there is evidence in our data of weak releases of this halocarbon. Comparison of our 2003 emission estimates with recent American and Canadian production and consumption figures implicates releases of banked materials as the predominant modern emission sources for these five regulated halocarbons in the two countries. Our large-scale measurement-based emission estimates can be used to improve estimates of the sizes and release rates of modern ODS banks in the United States and Canada, and perhaps in other developed nations. Improved estimates of the sizes and emission rates of ODS banks in developed countries will help to better constrain estimates of future global emissions and atmospheric halogen burdens, and hence, lead to more accurate projections of stratospheric ozone recovery.

[57] **Acknowledgments.** The COBRA-NA study was funded by the NASA Terrestrial Ecology Program, with additional resources from NOAA GMD and the NOAA Office of Global Programs, the NASA Upper Atmosphere Research and Atmospheric Chemistry Modeling and Analysis Programs, and the National Science Foundation Atmospheric Chemistry Program. We are indebted to the University of North Dakota for use of their Cessna Citation II aircraft, for extraordinarily skilled pilots Paul “Pipeline” LeHardy and Kevin Buettner, and for Tony Grainger and his suite of meteorological sensors aboard the aircraft. We are grateful for the aircraft and facilities support by the National Center for Atmospheric Research (NCAR) Research Aviation Facility at the Jefferson County Airport near Boulder, Colorado, and for general assistance by Pan Am Services at Pease Airport in Portsmouth, New Hampshire.

References

- Aucott, M. L., A. McCulloch, T. E. Graedel, G. Kleiman, P. Midgley, and Y.-F. Li (1999), Anthropogenic emissions of trichloromethane (chloroform, CHCl₃) and chlorodifluoromethane (HCFC-22): Reactive Chlorine Emissions Inventory, *J. Geophys. Res.*, *104*, 8405–8415.
- Bakwin, P. S., D. F. Hurst, P. P. Tans, and J. W. Elkins (1997), Anthropogenic sources of halocarbons, sulfur hexafluoride, carbon monoxide, and methane in the southeastern United States, *J. Geophys. Res.*, *102*, 15,915–15,925.
- Barnes, D. H., S. C. Wofsy, B. P. Fehla, E. W. Gottlieb, J. W. Elkins, G. S. Dutton, and S. A. Montzka (2003), Urban/industrial pollution for the New York City–Washington, D. C., corridor, 1996–1998: 2. A study of the efficacy of the Montreal Protocol and other regulatory measures, *J. Geophys. Res.*, *108*(D6), 4186, doi:10.1029/2001JD001117.
- Benkovitz, C. M., M. T. Scholtz, J. Pacyna, L. Tarrason, J. Dignon, E. C. Voldner, P. A. Spiro, J. A. Logan, and T. E. Graedel (1996), Global gridded inventories of anthropogenic emissions of sulfur and nitrogen, *J. Geophys. Res.*, *101*, 29,239–29,253.
- Cunnold, D. M., R. F. Weiss, R. G. Prinn, D. Hartley, P. G. Simmonds, P. J. Fraser, B. R. Miller, F. N. Alyea, and L. Porter (1997), GAGE/AGAGE

- measurements indicating reductions in global emissions of CCl_2F and CCl_2F_2 in 1992–1994, *J. Geophys. Res.*, *102*, 1259–1269.
- Daube, B. C., K. A. Boering, A. E. Andrews, and S. C. Wofsy (2002), A high-precision fast-response airborne CO_2 analyzer for in situ sampling from the surface to the middle stratosphere, *J. Atmos. Oceanic Technol.*, *19*, 1532–1543.
- Department of Energy (2004), Emissions of greenhouse gases in the United States 2003, *Rep. DOE/EIA-0573*, Washington, D. C.
- Derwent, R. G., P. G. Simmonds, S. O'Doherty, and D. B. Ryall (1998), The impact of the Montreal Protocol on halocarbon concentrations in Northern Hemisphere baseline and European air masses at Mace Head, Ireland over a ten year period from 1987–1996, *Atmos. Environ.*, *32*, 3689–3702.
- Ebel, A., R. Friedrich, and H. Rodhe (Eds.) (1997), *Transport and Chemical Transformation of Pollutants in the Troposphere*, vol. 7, *Tropospheric Modelling and Emission Estimation*, Springer, New York.
- Elkins, J. W., T. M. Thompson, T. H. Swanson, J. H. Butler, B. D. Hall, S. O. Cummings, D. A. Fisher, and A. G. Raffo (1993), Decrease in the growth rates of atmospheric chlorofluorocarbons 11 and 12, *Nature*, *364*, 780–783.
- Elkins, J. W., et al. (1996), Airborne gas chromatograph for in situ measurements of long-lived species in the upper troposphere and lower stratosphere, *Geophys. Res. Lett.*, *23*, 347–350.
- Environmental Protection Agency (EPA) (1993), *Regional Interim Emissions Inventories (1987–1991)*, vols. 1 and 2, Research Triangle Park, N. C.
- Environmental Protection Agency (EPA) (2003), Inventory of U.S. greenhouse gas emissions and sinks: 1990–2001, *Rep. EPA 430-R-03-004*, Washington, D. C.
- Environmental Protection Agency (EPA) (2004), Inventory of U.S. greenhouse gas emissions and sinks: 1990–2002, *Rep. EPA 430-R-04-003*, Washington, D. C.
- Environmental Protection Agency (EPA) (2005), Inventory of U.S. greenhouse gas emissions and sinks: 1990–2003, *Rep. EPA 430-R-05-003*, Washington, D. C.
- Fraser, P., D. Cunnold, F. Alyea, R. Weiss, R. Prinn, P. Simmonds, B. Miller, and R. Langenfelds (1996), Lifetime and emission estimates of 1,1,2-trichlorotrifluoroethane (CFC-113) from daily global background observations June 1982–June 1994, *J. Geophys. Res.*, *101*, 12,585–12,599.
- Fraser, P. J., D. E. Oram, C. E. Reeves, S. A. Penkett, and A. McCulloch (1999), Southern hemispheric halon trends (1978–1998) and global halon emissions, *J. Geophys. Res.*, *104*, 15,985–15,999.
- Geller, L. S., J. W. Elkins, J. M. Lobert, A. D. Clarke, D. F. Hurst, J. H. Butler, and R. C. Myers (1997), Tropospheric SF_6 : Observed latitudinal distribution and trends, derived emissions and interhemispheric exchange time, *Geophys. Res. Lett.*, *24*, 675–678.
- Gerbig, C., S. Schmitgen, D. Kley, A. Volz-Thomas, K. Dewey, and D. Haaks (1999), An improved fast-response vacuum-UV resonance fluorescence CO instrument, *J. Geophys. Res.*, *104*, 1699–1704.
- Gerbig, C., J. C. Lin, S. C. Wofsy, B. C. Daube, A. E. Andrews, B. B. Stephens, P. S. Bakwin, and C. A. Grainger (2003), Toward constraining regional-scale fluxes of CO_2 with atmospheric observations over a continent: 2. Analysis of COBRA data using a receptor-oriented framework, *J. Geophys. Res.*, *108*(D24), 4757, doi:10.1029/2003JD003770.
- Hurst, D. F., et al. (2004), Emissions of ozone-depleting substances in Russia during 2001, *J. Geophys. Res.*, *109*, D14303, doi:10.1029/2004JD004633.
- Intergovernmental Panel on Climate Change/Technology and Economic Assessment Panel (IPCC/TEAP) (2005), *Special Report on Safeguarding the Ozone Layer and the Global Climate System: Issues Related to Hydrofluorocarbons and Perfluorocarbons*, edited by B. Metz et al., 488 pp., Cambridge Univ. Press, New York.
- Khalil, M. A. K., R. M. Moore, B. D. Harper, J. M. Lobert, D. J. Erickson, V. Koropalov, W. T. Sturges, and W. C. Keene (1999), Natural emissions of chlorine-containing gases: Reactive Chlorine Emissions Inventory, *J. Geophys. Res.*, *104*, 8333–8346.
- Krol, M. C., J. Lelieveld, D. E. Oram, G. A. Sturrock, S. A. Penkett, C. A. M. Brenninkmeijer, V. Gros, J. Williams, and H. A. Scheeren (2003), Continuing emissions of methyl chloroform from Europe, *Nature*, *421*, 131–135.
- Li, J., D. M. Cunnold, H.-J. Wang, R. F. Weiss, B. R. Miller, C. Harth, P. Salameh, and J. M. Harris (2005), Halocarbon emissions estimated from Advanced Global Atmospheric Gases Experiment measured pollution events at Trinidad Head, California, *J. Geophys. Res.*, *110*, D14308, doi:10.1029/2004JD005739.
- Lin, J. C., C. Gerbig, S. C. Wofsy, A. E. Andrews, B. C. Daube, K. J. Davis, and C. A. Grainger (2003), A near-field tool for simulating the upstream influence of atmospheric observations: The Stochastic Time-Inverted Lagrangian Transport (STILT) model, *J. Geophys. Res.*, *108*(D16), 4493, doi:10.1029/2002JD003161.
- Lin, J. C., C. Gerbig, S. C. Wofsy, A. E. Andrews, B. C. Daube, C. A. Grainger, B. B. Stephens, P. S. Bakwin, and D. Y. Hollinger (2004), Measuring fluxes of trace gases at regional scales by Lagrangian observations: Application to the CO_2 Budget and Rectification Airborne (COBRA) study, *J. Geophys. Res.*, *109*, D15304, doi:10.1029/2004JD004754.
- Lobert, J. M., W. C. Keene, J. A. Logan, and R. Yevich (1999), Global chlorine emissions from biomass burning: Reactive Chlorine Emissions Inventory, *J. Geophys. Res.*, *104*, 8373–8390.
- Logan, J. A., M. J. Prather, S. C. Wofsy, and M. B. McElroy (1981), Tropospheric chemistry: A global perspective, *J. Geophys. Res.*, *86*, 7210–7254.
- Maiss, M., and C. A. M. Brenninkmeijer (1998), Atmospheric SF_6 : Trends, sources, and prospects, *Environ. Sci. Technol.*, *32*, 3077–3086.
- Maiss, M., L. P. Steele, R. J. Francey, P. J. Fraser, R. L. Langenfelds, N. Trivett, and I. Levin (1996), Sulfur hexafluoride: A powerful new atmospheric tracer, *Atmos. Environ.*, *30*, 1621–1629.
- McCulloch, A., and P. M. Midgley (2001), The history of methyl chloroform emissions: 1951–2000, *Atmos. Environ.*, *35*, 5311–5319.
- McCulloch, A., P. Ashford, and P. M. Midgley (2001), Historic emissions of fluorotrichloromethane (CFC-11) based on a market survey, *Atmos. Environ.*, *35*, 4387–4397.
- McCulloch, A., P. M. Midgley, and P. Ashford (2003), Releases of refrigerant gases (CFC-12, HCFC-22 and HFC-134a) to the atmosphere, *Atmos. Environ.*, *37*, 889–902.
- Midgley, P. M., and A. McCulloch (1995), The production and global distribution of emissions to the atmosphere of 1,1,1-trichloroethane (methyl chloroform), *Atmos. Environ.*, *29*, 1601–1608.
- Millet, D., and A. H. Goldstein (2004), Evidence for continuing methylchloroform emissions in the United States, *Geophys. Res. Lett.*, *31*, L17101, doi:10.1029/2004GL020166.
- Montzka, S. A., and P. J. Fraser (2003), Controlled substances and other source gases, in *Scientific Assessment of Ozone Depletion: 2002, Global Ozone Res. Monit. Proj. Rep. 47*, chap. 1, 498 pp., World Meteorol. Organ., Geneva.
- Montzka, S. A., J. H. Butler, R. C. Myers, T. M. Thompson, T. H. Swanson, A. D. Clarke, L. T. Lock, and J. W. Elkins (1996), Decline in the tropospheric abundance of halogen from halocarbons: Implications for stratospheric ozone depletion, *Science*, *272*, 1318–1322.
- Montzka, S. A., J. H. Butler, J. W. Elkins, T. M. Thompson, A. D. Clarke, and L. T. Lock (1999), Present and future trends in the atmospheric burden of ozone-depleting halogens, *Nature*, *398*, 690–694.
- Montzka, S. A., J. H. Butler, B. D. Hall, D. J. Mondeel, and J. W. Elkins (2003), A decline in tropospheric organic bromine, *Geophys. Res. Lett.*, *30*(15), 1826, doi:10.1029/2003GL017745.
- Morris, R. A., R. M. Miller, A. A. Viggiano, J. F. Paulson, S. Solomon, and G. Reid (1995), Effects of electron and ion reactions on atmospheric lifetimes of fully fluorinated compounds, *J. Geophys. Res.*, *100*, 1287–1294.
- Nedelec, P., V. Thouret, J. Brioude, B. Sauvage, J.-P. Cammas, and A. Stohl (2005), Extreme CO concentrations in the upper troposphere over northeast Asia in June 2003 from the in situ MOZAIC aircraft data, *Geophys. Res. Lett.*, *32*, L14807, doi:10.1029/2005GL023141.
- Olivier, J. G. J., J. A. Van Aardenne, F. Dentener, L. Ganzeveld, and J. A. H. W. Peters (2005), Recent trends in global greenhouse gas emissions: Regional trends and spatial distribution of key sources, in *Non- CO_2 Greenhouse Gases (NCGG-4)*, edited by A. Van Amstel, pp. 325–330, Millpress, Rotterdam, Netherlands.
- Palmer, P. I., D. J. Jacobs, L. J. Mickley, D. R. Blake, G. W. Sachse, H. E. Fuelberg, and C. M. Kiley (2003), Eastern Asian emissions of anthropogenic halocarbons deduced from aircraft concentration data, *J. Geophys. Res.*, *108*(D24), 4753, doi:10.1029/2003JD003591.
- Prather, M. J. (1985), Continental sources of halocarbons and nitrous oxide, *Nature*, *317*, 221–225.
- Press, W. H., S. A. Teukolsky, W. T. Vetterling, and P. B. Flannery (1992), *Numerical Recipes in C*, Cambridge Univ. Press, New York.
- Prinn, R. G., et al. (2000), A history of chemically and radiatively important gases in air deduced from ALE/GAGE/AGAGE, *J. Geophys. Res.*, *105*, 17,751–17,792.
- Prinn, R. G., et al. (2001), Evidence for substantial variations of atmospheric hydroxyl radicals in the past two decades, *Science*, *292*, 1882–1888.
- Romashkin, P. A., D. F. Hurst, J. W. Elkins, G. S. Dutton, D. W. Fahey, R. E. Dunn, F. L. Moore, R. C. Myers, and B. D. Hall (2001), In situ measurements of long-lived trace gases in the lower stratosphere by gas chromatography, *J. Atmos. Oceanic Technol.*, *18*, 1195–1204.
- Rudolph, J., K. von Czapiewski, and R. Koppmann (2000), Emissions of methyl chloroform (CH_3CCl_3) from biomass burning and the tropospheric methyl chloroform budget, *Geophys. Res. Lett.*, *27*, 1887–1890.

- Ryall, D. B., R. G. Derwent, A. J. Manning, P. G. Simmonds, and S. O'Doherty (2001), Estimating source regions of European emissions of trace gases from observations at Mace Head, *Atmos. Environ.*, *35*, 2507–2523.
- Simmonds, P. G., D. M. Cunnold, R. F. Weiss, R. G. Prinn, P. J. Fraser, A. McCulloch, F. N. Alyea, and S. O'Doherty (1998), Global trends and emissions estimates of CCl₄ from in situ background observations from July 1978 to June 1996, *J. Geophys. Res.*, *103*, 16,017–16,027.
- Thompson, T. M., et al. (2004), Halocarbons and other atmospheric trace species, in *Climate Monitoring and Diagnostics Laboratory Summary Report 2002–2003*, Rep. 27, chap. 5, 174 pp., Natl. Oceanic and Atmos. Admin., Boulder, Colo.
- United Nations Environment Programme (UNEP) (2002a), Production and consumption of ozone depleting substances under the Montreal Protocol 1986–2000, 77 pp., Nairobi.
- United Nations Environment Programme (UNEP) (2002b), Fourteenth meeting of the parties to the Montreal Protocol on substances that deplete the ozone layer, Rep. UNEP/OzL.Pro.14/3, 122 pp., Nairobi.
- United Nations Environment Programme (UNEP) (2003a), 2002 assessment report of the Halons Technical Options Committee, 69 pp., Nairobi.
- United Nations Environment Programme (UNEP) (2003b), Fifteenth meeting of the parties to the Montreal Protocol on substances that deplete the ozone layer, Rep. UNEP/OzL.Pro.15/4, 112 pp., Nairobi.
- United Nations Environment Programme (UNEP) (2004), Sixteenth meeting of the parties to the Montreal Protocol on substances that deplete the ozone layer, Rep. UNEP/OzL.Pro.16/4, 110 pp., Nairobi.
- United Nations Environment Programme (UNEP) (2005), Seventeenth meeting of the parties to the Montreal Protocol on substances that deplete the ozone layer, Rep. UNEP/OzL.Pro.17/6, 105 pp., Nairobi.
-
- B. C. Daube, D. M. Matross, and S. C. Wofsy, Department of Earth and Planetary Sciences, Harvard University, 20 Oxford Street, Cambridge, MA 02138, USA.
- J. W. Elkins, B. D. Hall, and D. F. Hurst, Global Monitoring Division, NOAA Earth System Research Laboratory, 325 Broadway R/GMD1, Boulder, CO 80305, USA. (dale.hurst@noaa.gov)
- C. Gerbig, Max Planck Institute for Biogeochemistry, Hans-Knöll-Straße 10, D-07745 Jena, Germany.
- J. C. Lin, Department of Earth Sciences, University of Waterloo, Waterloo, ON, Canada N2L 301.
- P. A. Romashkin, Research Aviation Facility, National Center for Atmospheric Research, 10802 Airport Court, Broomfield, CO 80021-2561, USA.